A Letters Journal Exploring the Frontiers of Physics

October 2009

EPL, **88** (2009) 26004
doi: 10.1209/0295-5075/88/26004

www.epljournal.org

Effect of substrate on thermal conductivity of single-walled carbon nanotubes

A. V. Savin[1,2(a)], Y. S. Kivshar[2] and B. Hu[3,4]

[1] *Semenov Institute of Chemical Physics, Russian Academy of Sciences - Moscow 119991, Russia*
[2] *Nonlinear Physics Center, Research School of Physics and Engineering, Australian National University Canberra, ACT 0200, Australia*
[3] *Department of Physics and Center for Nonlinear Studies, Hong Kong Baptist University - Hong Kong, China*
[4] *Department of Physics, University of Houston - Houston, TX 77204-5005, USA*

received 10 June 2009; accepted in final form 9 October 2009
published online 9 November 2009

PACS 65.80.+n – Thermal properties of small particles, nanocrystals, and nanotubes
PACS 63.22.Gh – Nanotubes and nanowires

Abstract – We analyze numerically the thermal conductivity of single-walled carbon nanotubes placed on a flat rigid substrate. We demonstrate that the character of thermal conductivity depends crucially on the interaction between the nanotube and the substrate. In particular, we reveal that unlike the well-established anomalous thermal conductivity of isolated carbon nanotubes, the nanotube placed on a substrate demonstrates *normal thermal conductivity* due to the appearance of a narrow gap in the frequency spectrum of acoustic phonons.

Carbon-based structures display the highest measured thermal conductivity of any known material at moderate temperatures. The discovery of carbon nanotubes (CNTs) in 1991 [1] has led to suggestions that this new material could have a thermal conductivity greater than that of diamond and graphite [2]. Experimental data [3] demonstrated that conductivity of CNTs at room temperature can exceed the value of 3000 W/mK which is two orders of magnitude larger than the estimates of earlier experiments that used macroscopic mat samples. Further studies employing different experimental methods confirmed that CNTs demonstrate anomalously high thermal conductivity. However, recent experiments [4] which measured the dependence of thermal conductivity on the length of individual single-walled CNTs placed on a Si substrate, revealed that the coefficient of thermal conductivity saturates for longer nanotubes. This observation contradicts earlier theoretical results based on the molecular-dynamics simulations [5–10]. Therefore, a natural question arises: *What is the effect of the substrate on the thermal conductivity of single-walled carbon nanotubes?*

In this letter, we study numerically a transfer of thermal energy along an isolated single-walled CNT and analyze the effect of a rigid substrate on the character of thermal conductivity and its dependence on the nanotube length. We employ two different methods: i) a direct modeling of the heat transfer by means of the molecular-dynamics simulations, and ii) the study of the equilibrium multi-particle dynamics based on the Green-Kubo formalism. We demonstrate that fixing a nanotube on a substrate changes dramatically its thermal conductivity. The nanotube placed on a flat rigid surface displays a finite conductivity, in a sharp contrast to an isolated CNT that displays anomalous thermal conductivity.

For modeling thermal conductivity of long nanotubes, we consider the nanotubes with the indices $(m, 0)$ (zigzag CNT) and (m, m) (armchair CNT). Figure 1(a) shows schematically a nanotube placed on a flat rigid surface (*e.g.*, a surface of Si crystal [4]). It is convenient to describe the structure of an ideal nanotube as that created by an operation of screw rotation by an elementary unit cell defined between two neighboring carbon atoms located at the surface of the cylindrical tube. We introduce such a operator as $S(\Delta z, \delta\varphi)$, that moves the point with the cylindrical coordinates (z, φ) to the point with the coordinates $(z + \Delta z, \varphi + \delta\varphi)$, *i.e.* a shift along the axis by the distance Δz and its rotation by the angle $\delta\varphi$. This operation is commutative, *i.e.* any two operators $S_1 = S(\Delta z_1, \delta\varphi_1)$ and $S_2 = S(\Delta z_2, \delta\varphi_2)$ are linearly independent. The operation $S_1^m S_2^n$ means the transformation of

(a) E-mail: asavin@center.chph.ras.ru

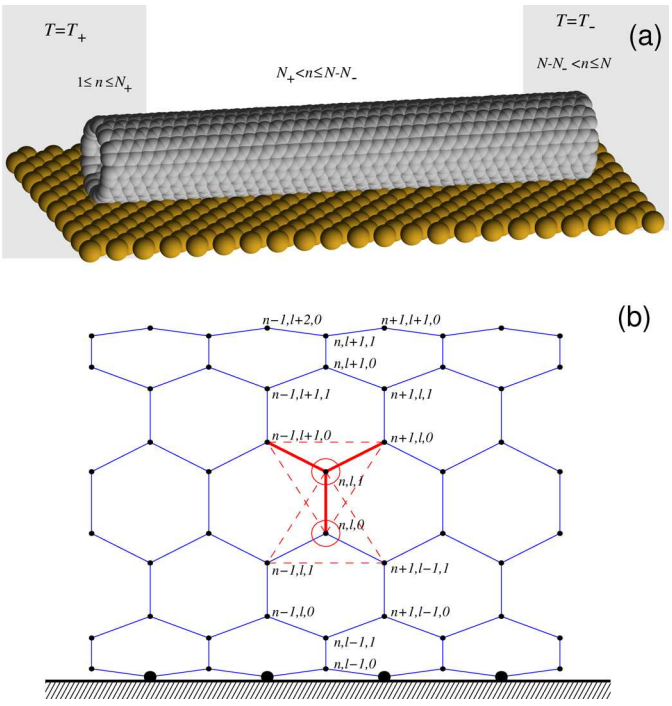

Fig. 1: (Colour on-line) (a) Examples of armchair CNT (10,10) on a substrate, N —number of longitudinal steps. First left N_+ segments attached to the $T = T_+$ thermostat and last right N_- segments attached to the $T = T_-$ thermostat. (b) Schematics of armchair CNT and numbering of atoms. Thick red lines mark valent bond couplings, thin red arcs mark valent angle couplings, thin dashed lines show the foundation of two pyramids which form dihedral angles along the valent bonds in the elementary cell (n, l). Larger balls show the atoms which are fixed for including the interaction with a substrate.

the coordinates according to the relation: $(z, \varphi) \to (z + m\Delta z_1 + n\Delta z_2, \varphi + m\delta\varphi_1 + n\delta\varphi_2)$. The minimum values of the non-negative numbers m and n when the operator reduces to the unit operator are called the indices of the nanotube chirality.

For the nanotube with the index (m, m) shown in fig. 1(b) the first operator is reduced to a rotation by the angle $\delta\varphi_1 = 2\pi/m$ (because the shift is zero, $\Delta z_1 = 0$), and the second operator defines the shift by the value $\Delta z_2 > 0$ and rotation by the angle $\delta\varphi_2 = \pi/m$. Therefore, each atom of carbon can be numerated by three indices (n, l, k), where the first two indices $n = 0, \pm1, \pm2, \ldots$, $l = 0, 1, \ldots, m-1$ define the number of the elementary cell (the cell with the number (n, l) is obtained from the cell $(0, 0)$ by applying the operator $S_1^l S_2^n$), and the third index $k = 0, 1$ stands for number of atoms in the cell. In equilibrium, the nanotube is characterized by the following parameters: radius R_0, angular shift φ_0, and longitudinal shift h. In the equilibrium state, the atoms have the coordinates

$$\begin{aligned} x^0_{n,l,0} &= h(n-1), & x^0_{n,l,1} &= h(n-1), \\ y^0_{n,l,0} &= R\cos(\phi_{n,l,0}), & y^0_{n,l,1} &= R\cos(\phi_{n,l,1}), \\ z^0_{n,l,0} &= R\sin(\phi_{n,l,0}), & z^0_{n,l,1} &= R\sin(\phi_{n,l,1}), \end{aligned} \quad (1)$$

where the cylindrical angles are $\phi_{n,l,0} = [l - 1 + (n-1)/2]\Delta\phi$, $\phi_{n,l,1} = \phi_{n,l,0} + \varphi$, and the angular step is $\Delta\phi = 2\pi/m$.

To study the thermodynamics of the nanotube, we present the system Hamiltonian in the form

$$H = \sum_n h_n = \sum_n \sum_{l=0}^{m-1} \left[\frac{1}{2}M(\dot{\mathbf{u}}^2_{n,l,0} + \dot{\mathbf{u}}^2_{n,l,1}) + P_{n,l}\right], \quad (2)$$

where $M = 12 \times 1.6603 \cdot 10^{-27}$ kg is the mass of the carbon atom, $\mathbf{u}_{n,l,k} = (x_{n,l,k}(t), y_{n,l,k}(t), z_{n,l,k}(t))$ is the radius vector describing the position of the atom with the indices (n, l, k) at time t. The term $P_{n,l}$ describes the interaction energy of the atoms in the cell (n, l) with the atoms of the neighboring cells.

In almost all papers devoted to the numerical study of the thermal properties of carbon nanotubes, an effective interatomic interaction was described by the Brenner potential [11,12]. The Brenner potential allows modeling the formation and breakup of molecular structures, as well as breakdown and formation of valent bonds. However, since at the room temperatures the nanotube structure does not change, for the study of thermal conductivity we may employ simpler standard potentials of the intermolecular interaction which are used in the molecular-dynamics simulations of the dynamics of large macromolecules. In this case, for the armchair CNT (see fig. 1(b)), the energy of the interaction between the neighboring cells can be presented in the form

$$\begin{aligned} P_{n,l} &= V(\mathbf{u}_{n,l,0}, \mathbf{u}_{n,l,1}) + V(\mathbf{u}_{n,l,1}, \mathbf{u}_{n+1,l,0}) \\ &+ V(\mathbf{u}_{n,l,1}, \mathbf{u}_{n-1,l+1,0}) + U(\mathbf{u}_{n-1,l,1}, \mathbf{u}_{n,l,0}, \mathbf{u}_{n+1,l-1,1}) \\ &+ U(\mathbf{u}_{n-1,l,1}, \mathbf{u}_{n,l,0}, \mathbf{u}_{n,l,1}) \\ &+ U(\mathbf{u}_{n+1,l-1,1}, \mathbf{u}_{n,l,0}, \mathbf{u}_{n,l,1}) + U(\mathbf{u}_{n,l,0}, \mathbf{u}_{n,l,1}, \mathbf{u}_{n-1,l+1,0}) \\ &+ U(\mathbf{u}_{n,l,0}, \mathbf{u}_{n,l,1}, \mathbf{u}_{n+1,l,0}) \\ &+ U(\mathbf{u}_{n-1,l+1,0}, \mathbf{u}_{n,l,1}, \mathbf{u}_{n+1,l,0}) \\ &+ W(\mathbf{u}_{n,l,1}, \mathbf{u}_{n,l,0}, \mathbf{u}_{n-1,l,1}, \mathbf{u}_{n+1,l-1,1}) \\ &+ W(\mathbf{u}_{n,l,1}, \mathbf{u}_{n,l,0}, \mathbf{u}_{n+1,l-1,1}, \mathbf{u}_{n-1,l,1}) \\ &+ W(\mathbf{u}_{n-1,l,1}, \mathbf{u}_{n,l,0}, \mathbf{u}_{n,l,1}, \mathbf{u}_{n+1,l-1,1}) \\ &+ W(\mathbf{u}_{n,l,0}, \mathbf{u}_{n,l,1}, \mathbf{u}_{n-1,l+1,0}, \mathbf{u}_{n+1,l,0}) \\ &+ W(\mathbf{u}_{n,l,0}, \mathbf{u}_{n,l,1}, \mathbf{u}_{n+1,l,0}, \mathbf{u}_{n-1,l+1,0}) \\ &+ W(\mathbf{u}_{n+1,l,0}, \mathbf{u}_{n,l,1}, \mathbf{u}_{n,l,0}, \mathbf{u}_{n-1,l+1,0}), \end{aligned}$$

where the first potential $V(\mathbf{u}_1, \mathbf{u}_2)$ describes the deformation energy of a valent bond created by two carbon atoms with the coordinates $\mathbf{u}_1$ and $\mathbf{u}_2$, the second potential $U(\mathbf{u}_1, \mathbf{u}_2, \mathbf{u}_3)$ stands for the deformation energy of a plane valent angle created by three atoms with the coordinates $\mathbf{u}_1$, $\mathbf{u}_2$, and $\mathbf{u}_3$, and the third potential $W(\mathbf{u}_1, \mathbf{u}_2, \mathbf{u}_3, \mathbf{u}_4)$ describes the deformation energy of the angle formed by two planes $\mathbf{u}_1\mathbf{u}_2\mathbf{u}_3$ and $\mathbf{u}_2\mathbf{u}_3\mathbf{u}_4$. Similarly, we can

construct the Hamiltonian for the zigzag CNT with the chirality $(m, 0)$ [13,14].

In our numerical studies we use the interaction potentials usually employed for modeling the dynamics of large macromolecules. The details of the potentials V, U, W can be found in ref. [13]. For comparison, we also study the same model with the interactions described by the Brenner potentials [11,12]. In this later case, the interaction of the n-th atom with its three neighbors is described by a sum of three Brenner potentials.

We consider single-walled CNT with chirality (m, m). We define the six-dimensional vector $\mathbf{x}_{n,l} = (x_{n,l,0}, y_{n,l,0}, z_{n,l,0}, x_{n,l,1},\ y_{n,l,1}, z_{n,l,1})$ which determines the atom coordinates of an elementary cell (n, l), and then in Hamiltonian (2) function $P_{n,l} = P(\mathbf{x}_{n-1,l}, \mathbf{x}_{n-1,l+1}, \mathbf{x}_{n,l}, \mathbf{x}_{n+1,l-1}, \mathbf{x}_{n+1,l})$. Hamiltonian (2) generates the system of equations of motion $M\ddot{\mathbf{x}}_{n,l} = P_{1,n+1,l} + P_{2,n+1,l-1} + P_{3,n,l} + P_{4,n-1,l+1} + P_{5,n-1,l}$, where the function $P_{j,n,l} = Q_j(x_{n-1,l}, x_{n-1,l+1}, x_{n,l},\ x_{n+1,l-1}, \mathbf{x}_{n+1,l})$, $Q_j = \partial P(\mathbf{x}_1, \mathbf{x}_2, \ldots, \mathbf{x}_5)/\partial \mathbf{x}_j, j = 1, 2, \ldots, 5$.

Local heat flux through the n-th cross-section, j_n, determines a local longitudinal energy density h_n by means of a discrete continuity equation, $\dot{h}_n = j_n - j_{n+1}$. Using the energy density from eq. (2) and the motion equations, we obtain the general expression for the energy flux through the n-th cross-section of the nanotube, $j_n = \sum_{l=0}^{m-1} [(P_{1,n,l} + P_{2,n,l-1})\dot{\mathbf{x}}_{n-1,l} - (P_{4,n-1,l+1} + P_{5,n-1,l})\dot{\mathbf{x}}_{n,l}]$.

For a direct modeling of the heat transfer along the nanotube, we consider a nanotube of a fixed length Nh with fixed ends. We place the first $N_+ = 40$ steps into the Langevin thermostat at $T_+ = 310\,\mathrm{K}$, and the last $N_- = 40$ steps, into the thermostat at $T_- = 290\,\mathrm{K}$. We select the initial conditions corresponding to the ground state of the nanotube, and solve the equations of motion numerically tracing the transition to the regime with the stationary heat flux. At the inner part of the nanotube $(N_+ < n \leqslant N - N_-)$, we observe the formation of a temperature gradient corresponding to a constant flux. The distribution of the average values of temperature and heat flux along the nanotube can be found in the form, $T_n = \lim_{t\to\infty} \frac{M}{6mk_B t} \int_0^t \sum_{l=0}^{m-1} \dot{\mathbf{x}}_{n,l}^2(\tau)\,\mathrm{d}\tau$, $J_n = \lim_{t\to\infty} \frac{h}{t} \int_0^t j_n(\tau)\mathrm{d}\tau$, where k_B is the Boltzmann constant.

The distribution of the temperature and local heat flux along the nanotube are shown in fig. 2. The heat flux in each cross-section of the inner part of the nanotube should remain constant, namely $J_n \equiv J$ for $N_+ < n \leqslant N - N_-$. The requirement of independence of the heat flux J_n from a local position n is a good criterion for the accuracy of numerical simulations, as well as it may be used to determine the integration time for calculating the mean values of J_n and T_n. As follows from the figure, the heat flux remains constant along the central inner part of the nanotube.

We notice that an effective heat resistance appears at the interface between the central part of the nanotube and its edge placed in thermostat. The thermal resistance originates only from the thermostat and its "viscosity" can be characterized by the relaxation time t_r. Our numerical simulations demonstrate that the thermal conductivity and the temperature profile in the central part of the nanotube depend very weakly on the relaxation time. In particular, for $t_r = 0.4,\ 0.2,\ 0.1,\ 0.05$ and $0.025\,\mathrm{ps}$ this change does not exceed a few percents. Therefore, a linear temperature gradient can be used to define the local coefficient of thermal conductivity, $\kappa(N') = (N' - 1)J/(T_{N_+ + 1} - T_{N - N_-})S$, where $N' = N - N_+ - N_-$ and $S = \pi R^2$ is the area of the cross-section, R is the radius of the nanotube. Using this definition, we calculate the asymptotic value of the coefficient $\kappa = \lim_{N\to\infty} \kappa(N)$.

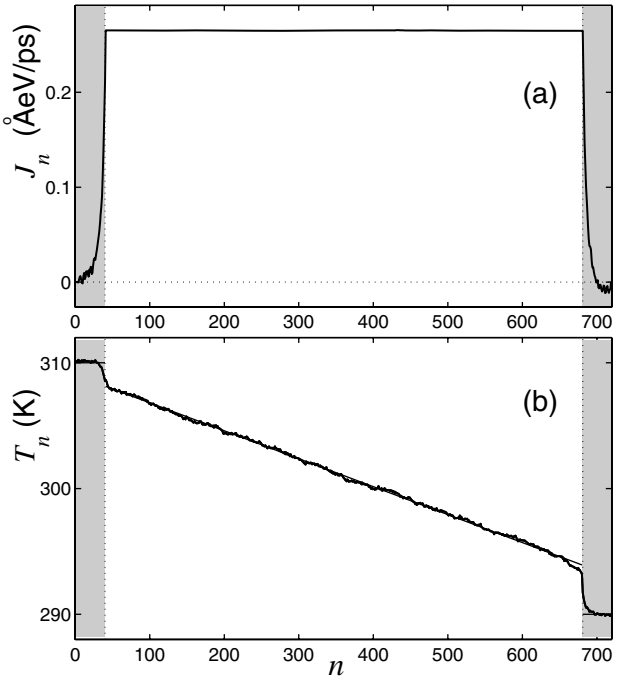

Fig. 2: Distributions of (a) local heat flux J_n and (b) local average temperatures T_n along armchair CNT (6,6). The length of the nanotube is $L = Nh = 88.7\,\mathrm{nm}$ ($N = 720$, $h = 0.123\,\mathrm{nm}$), temperatures are $T_+ = 310\,\mathrm{K}$ and $T_- = 290\,\mathrm{K}$, the numbers of end steps interacting with the thermostats $N_\pm = 40$ (corresponding fragments are shown in grey). The averaging time is $t = 10\,\mathrm{ns}$, and the relaxation time of the Langevin thermostat is $t_r = 0.1\,\mathrm{ps}$.

An alternative way to study thermal conductivity is based on the well-known Green-Kubo formula [15]

$$\kappa = \frac{h^2}{k_B T^2} \lim_{t\to\infty} \int_0^t \lim_{N\to\infty} \frac{1}{V} \langle \mathbf{J}(s) \cdot \mathbf{J}(0) \rangle \mathrm{d}s, \qquad (3)$$

where $V = \pi h R^2 N$ is an effective volume of the nanotube with the length Nh, and $\mathbf{J} = \sum_{n=1}^{N} j_n$ is the total heat flux along the finite-length nanotube with periodic boundary

conditions. Formula (3) can be presented in the form

$$\kappa = \frac{h}{k_B T^2 \pi R^2} \lim_{t\to\infty} \int_0^t C(s)\mathrm{d}s, \qquad (4)$$

where we introduce the flux-flux correlation function $C(t) = \lim_{N\to\infty}\langle \mathbf{J}(t)\cdot\mathbf{J}(0)\rangle/N$, and the averaging $\langle\cdot\rangle$ is performed over all thermal states of the nanotube.

For employing the latter approach we should calculate numerically the integral (4). If this integral diverges, we conclude that the nanotube possesses infinite thermal conductivity. Numerically, we calculate the correlation function $C(t)$ for a finite-length chain, $C_N(t) = \langle \mathbf{J}(s)\cdot\mathbf{J}(s-t)\rangle_s/N$, and then take a large enough number of the cells N in order to approximate the correlation function by the function $C_N(t)$. We require that the correlation function does not change for the time interval $[0,t]$ when we increase the nanotube length into two times. Then for this time interval the function $C_N(t)$ should coincide with the function $C(t)$. Our numerical results demonstrate that it is necessary to take $N = 2000$ for the nanotube with chirality $(m,0)$, but the nanotube with chirality (m,m) requires the value $N = 3000$.

To find the correlation function, we solve numerically a system of equations of motion that follow from the Hamiltonian (2) with periodic boundary conditions and initial conditions corresponding to a thermalized state of nanotube at the temperature $T = 300\,\mathrm{K}$. To increase the accuracy of these calculations, we average the data for 10^3 independent realizations of different thermal states of the nanotube.

The form of the correlation function $C(t)$ depends substantially on the nanotube chirality (see fig. 3). For example, for the nanotube with chirality (m,m) this function does not display any high-frequency oscillations, after abound 0.4 ps oscillations decay rapidly, and then the function tends to zero monotonically for $t\to\infty$. For the nanotube with the index $(m,0)$, we observe always high-frequency oscillations for $t < 3\,\mathrm{ps}$. However, these oscillations decay for longer time and the function becomes monotonically decaying for $t\to\infty$.

The flux-flux correlational function calculated for an isolated nanotube always vanishes in accord with the power law, $C(t)\sim t^{-\alpha}$, where the index $\alpha < 1$ (see fig. 3(b)). The value of α grows monotonously with the nanotube radius, but it remains smaller than unity. For the nanotubes with the indices (3,3) and (5,0) (radius $R = 2\,\text{Å}$) we find $\alpha = 0.5$, whereas for the nanotubes (6,6) and (10,0) (radius $R = 4\,\text{Å}$), this power is $\alpha = 0.7$, and it is $\alpha = 0.9$ for the nanotube (20,0) (radius $R = 8\,\text{Å}$). From these results it follows that the integral in the Green-Kubo formula (4) diverges, so that thermal conductivity of CNT tends to infinity. This result has been verified by the direct modeling of the heat transfer.

The dependence of the coefficient of thermal conductivity κ on the length of the nanotube is presented in figs. 4(a) and (b). As follows from these results, the coefficient κ grows as L^β, whereas the growth speed depends

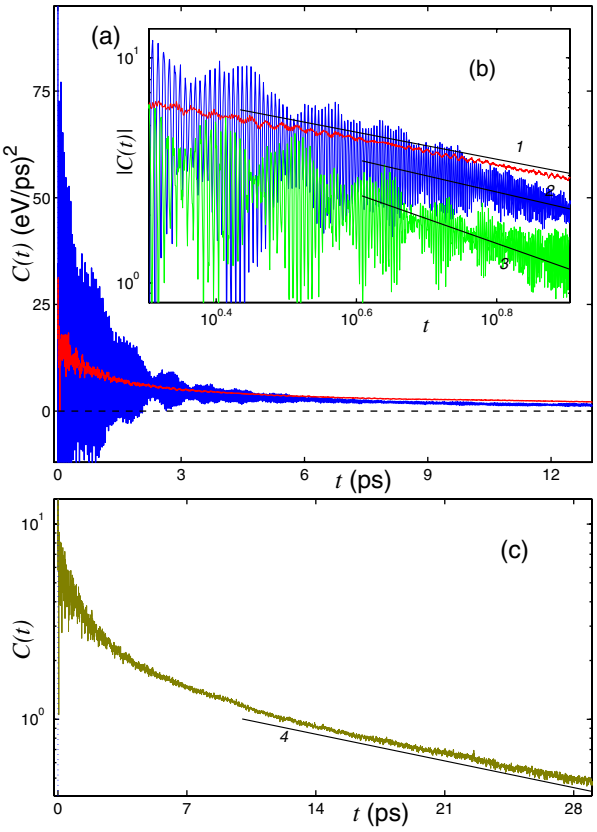

Fig. 3: (Colour on-line) (a) Dependence of the correlation function $C(t)$ of an isolated CNT (3,3) (red curve) and (10,0) (blue curve). (b) Power dependence of the correlation function of an isolated CNT (3,3) (red curve 1), (10,0) (blue curve 2) and the CNT nanotube (10,0) fixed on a substrate (green curve 3). Straight lines show the dependence $t^{-\alpha}$ with the powers $\alpha =$ 0.50, 0.72, 1.1 (lines 1, 2, and 3). (c) Exponential decay of the correlation function $C(t)$ for the nanotube CNT (3,3) fixed on a substrate (curve 4), the solid line show the dependence $\exp(-\alpha t)$ with $\alpha = 0.045$. Temperature $T = 300\,\mathrm{K}$.

on the nanotube radius R but not on its chirality. For the nanotubes of different chirality but approximately similar radii, *e.g.* the nanotubes (3,3) and (5,0), (6,6) and (10,0) the coefficient κ grows with the similar speed, namely $\beta = 0.38$ for $R = 2\,\text{Å}$, and $\beta = 0.21$ for $R = 4\,\text{Å}$. Thus, for large enough values of L the nanotubes of the same radius have the same value of the thermal conductivity coefficient.

In order to model thermal conductivity of a nanotube placed on a flat rigid substrate (*e.g.* a surface of the Si crystal), we fix the atoms which touch the surface (see fig. 1(a)). Fixing only a single atom in each of the n-th transverse layer of the nanotube leads to the disappearance of long-wave acoustic phonons and to the appearance of a narrow gap $[0,\omega_0]$ at the bottom of the frequency spectrum of small-amplitude oscillations. For example, for the nanotube (3,3) the gap width is $\omega_0 = 131\,\mathrm{cm}^{-1}$, for the nanotube (6,6), it is $\omega_0 = 94\,\mathrm{cm}^{-1}$, and for the nanotube (12,12), $\omega_0 = 41\,\mathrm{cm}^{-1}$. Fixing a

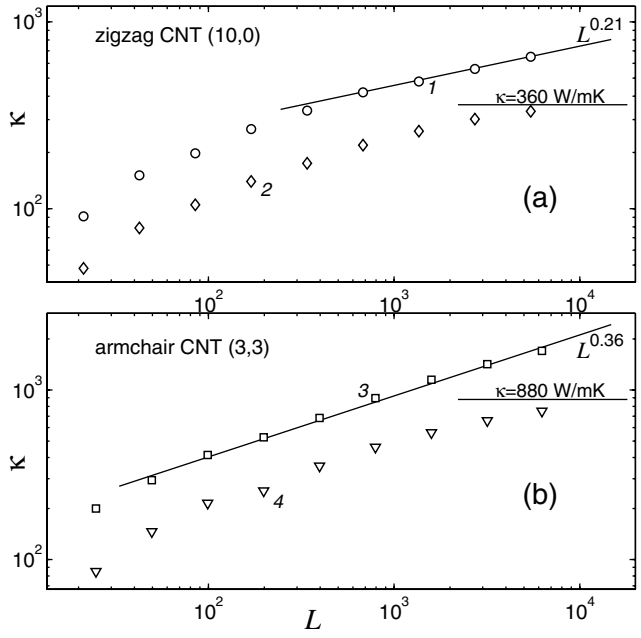

Fig. 4: Dependence of the coefficient of thermal conductivity κ on the nanotube length L for (a) zigzag CNT (10,0) and (b) armchair CNT (3,3). Symbols 1 and 3 mark the dependences calculated for isolated nanotubes, while the symbols 2 and 4 mark the corresponding dependences for the nanotube placed on a substrate. Straight lines show the dependence $\kappa = L^{\alpha}$. Functions are measured in the units of: $[\kappa] = \mathrm{W/mK}$ and $[L] = \text{Å}$.

zigzag nanotube gives a smaller frequency gap, namely $\omega_0 = 75\,\mathrm{cm}^{-1}$ for CNT (5,0), $22\,\mathrm{cm}^{-1}$ for the nanotube (10,0) and $6\,\mathrm{cm}^{-1}$, for the nanotube (20,0).

The appearance of a gap in the frequency spectrum leads to a dramatic change of the character of thermal conductivity, see fig. 4. For small values of the nanotube length L, the thermal conductivity coefficient κ decreases in two times. When L grows, the growth of the conductivity coefficient slows down, and we expect that the dependence $\kappa(L)$ should saturate for large L. This is confirmed by the behavior of the correlational function $C(t)$ which decays faster than t^{-1} after fixing the nanotube on a substrate.

For zigzag CNT (10,0), the correlation function decays for $t \to \infty$ as $t^{-1.05}$ (see fig. 3(b)). For larger time it is hard to find an explicit asymptotic dependence. However, for the exponential approximation the Green-Kubo formula (4) gives the value $\kappa = 360\,\mathrm{W/mK}$, while for the power law this value becomes $\kappa = 990\,\mathrm{W/mK}$. According to fig. 4(a), the former value looks more realistic. For numerical modeling, a nanotube of a smaller radius is more convenient to study, so we consider the nanotube $(3,3)$. For this case, we obtain numerically the dependence $C(t)$ for large t in the form $\exp(-\alpha t)$ with $\alpha = 0.045\,\mathrm{ps}^{-1}$ (see fig. 3(c)). For this latter case the Green-Kubo formula (4) gives the coefficient $\kappa = 880\,\mathrm{W/mK}$. As follows from fig. 4(b), this result agrees well with the convergence of the series $\kappa(N)$ for $N \to \infty$. Therefore, the interaction with a substrate changes not only the value of nanotube thermal conductivity but also the character of this dependence on the length of the nanotube showing saturation for large lengths.

In our analysis presented above we used the simplest model for describing the interaction between a nanotube and the substrate. In order to model this interaction more rigorously, *e.g.* describing the interaction with the Si substrate, we may expand the model substantially, *e.g.* by taking into account the finite thermal conductivity of the substrate and a heat exchange between the nanotube and substrate in each part of the CNT. In a general model, more atoms will be interacting with a substrate and none of the atoms is fixed. However, the main result about the appearance of a spectral gap and its dramatic effect on the thermal conductivity will not change, the only thing that will change is the value of the zero-k gap. In addition, this effect will be modified by the finite thermal conductivity of the substrate. Therefore, we considered the simplest model that reflects correctly the physics of this effect. In addition, the effect does not depend much on the type of the potentials used. Taking into account other effects including a finite conductivity of the substrate will modify only the value of the thermal conductivity coefficient, but it will neither change the physics nor major predictions.

Comparing our numerical results for the thermal conductivity with the theoretical models [16,17] that describe the transition between diffusion and ballistic regimes in nanoscale structures, we come to the conclusion that for the nanotube we studied here the mean free path of heat carries is of the same order or larger than the nanotube length, and for the Knudsen number, $Kn > 1$.

In summary, we have revealed that the interaction of carbon nanotubes with a substrate can change dramatically the character of thermal conductivity, due to the appearance of a narrow gap at the bottom of the frequency spectrum of acoustic phonons. We believe our results may be useful for the experimental studies of carbon nanotubes under various conditions.

* * *

AVS acknowledges the support from the Hong Kong Baptist University and the Australian Research Council. The authors thank the Joint Supercomputer Center of the Russian Academy of Sciences for using computer facilities.

REFERENCES

[1] Iijima S., *Nature*, **354** (1991) 56.
[2] Hone J., Whitney M., Piskoti C. and Zettl A., *Phys. Rev. B*, **59** (1991) 2514.
[3] Kim P., Shi L., Majumdar A. and McEuen P., *Phys. Rev. Lett.*, **87** (2001) 215502.

[4] Wang Z. L., Tang D. W., Li X. B., Zheng X. H., Zhang W. G., Zheng L. X., Zhu Y. T., Jin A. Z., Yang H. F. and Gu C. Z., *Appl. Phys. Lett.*, **91** (2007) 123119.
[5] Maruyama S., *Physica B*, **323** (2002) 187.
[6] Maruyama S., *Microscale Thermophys. Eng.*, **7** (2003) 41.
[7] Zhang G. and Li B., *J. Chem. Phys.*, **123** (2005) 114714.
[8] Wanga J. and Wang J.-S., *Appl. Phys. Lett.*, **88** (2006) 111909.
[9] Shiomi J. and Maruyama S., *Phys. Rev. B*, **73** (2006) 205420.
[10] Shiomi J. and Maruyama S., *Jpn. J. Appl. Phys.*, **47** (2008) 2005.
[11] Brenner D. W., *Phys. Rev. B*, **42** (1990) 9458.
[12] Brenner D. W., Shenderova O. A., Harrison J. A., Stuart S. J., Ni B. and Sinnott S. B., *J. Phys.: Condens. Matter*, **14** (2002) 783.
[13] Savin A. V. and Kivshar Y. S., *EPL*, **82** (2008) 66002.
[14] Savin A. V. and Kivshar Y. S., *Appl. Phys. Lett.*, **94** (2009) 111903.
[15] Kubo R., Toda M. and Hashitsume N., *Solid State Sci.*, **31** (1991) 185.
[16] Lebon G., Jou D. and Casas-Vazquez J., *Understanding Non-equilibrium Thermodynamics. Foundations Applications Frontiers* (Springer) 2008, p. 331.
[17] Alvarez X. and Jou D., *Appl. Phys. Lett.*, **90** (2007) 083109.